CHEMISTRY
A EUROPEAN JOURNAL

ChemPubSoc Europe

DOI: 10.1002/chem.201301917

Effect of Cation–π Interactions and Steric Bulk on the Catalytic Action of Oxidosqualene Cyclase: A Case Study of Phe728 of β-Amyrin Synthase from *Euphorbia tirucalli* L

Ryousuke Ito,[a] Ippei Hashimoto,[a] Yukari Masukawa,[a] and Tsutomu Hoshino*[a, b]

Abstract: The function of the active-site residues of oxidosqualene cyclases (OSCs) has been presumed mainly in light of the product distribution; however, not much research has been performed into the enzymatic activity of mutated OSCs. β-Amyrin, which is widely found in the plant kingdom, is classified as an OSC; mutational studies on β-amyrin cyclase are very limited. Six site-specific mutations targeted at the Phe728 residue of *Euphorbia tirucalli* β-amyrin synthase (EtAS) were constructed to inspect the function of this aromatic residue. We developed a simple method to evaluate the in vivo enzymatic activity; the expression levels of EtASs and the quantities of the cyclic triterpenes produced were determined by use of western blot and GC analyses, respectively. Measurement of the relative in vivo activity of the mutants versus that of the wild-type enzyme showed that the Ala, Met, His, and Trp variants had significantly decreased activity, but that the Tyr mutant had a high activity, which was nearly the same as that of the wild-type enzyme. In contrast to Tyr, Ala and Met possess no π-electrons; thus, the role of Phe728 is to stabilize the cationic intermediates, resulting in facilitation of the ring-expansion processes, especially by stabilizing the secondary cations. The decreased activity of the Trp mutant is ascribed to the introduction of a large steric bulk, leading to looser binding of oxidosqualene in the Trp variant. The His mutant afforded germanicol as the main product, indicating that the Phe residue is located near the D/E-ring-formation site. Changes in the steric bulk gave some cationic intermediates, resulting in the formation of 13 cyclic triterpenes, including an unnatural triterpene, (17*E*)-dammara-17(20),24-dien-3β-ol, and isoursenol, which has rarely been found in nature. In this study, we provide the first experimental evidence that cation–π interactions play a key role in the catalytic action of OSCs.

Keywords: alkenes · cyclization · enzyme catalysis · polycycles · terpenoids

Introduction

Triterpenes are abundant in nature and have important biological functions. Polycyclic triterpenes, including steroid scaffolds, are biosynthesized through ring-forming reactions (polycyclization) of linear molecules of either squalene or 2,3-oxidosqualene (**1**), with a C_{30} chain.[1] The structural diversity of triterpene skeletons is remarkable;[2] well-known triterpenes include lanosterol from vertebrates and fungi, cycloartenol and α- and β-amyrin from plants, and hopene from prokaryotes. The polycyclization reactions proceed with complete regio- and stereospecificity, leading to the formation of new C–C bonds and chiral centers, with four C–C bonds and seven chiral centers in the lanostane skeleton, five C–C bonds and nine stereocenters in hopanoid, and five C–C bonds and eight chiral centers in β-amyrin (Scheme 1). This intriguing biosynthetic mechanism catalyzed by oxidosqualene cyclase (OSC) is a fascinating research area for chemists and biologists alike.

Site-directed mutagenesis experiments have been used to investigate the catalytic function of the active-site residues in lanosterol synthase from *Saccharomyces cerevisiae*,[1e,3] plant and fungal triterpene synthases from *Arabidopsis thaliana* and other species,[4,5] and hopene synthase from *Alicyclobacillus acidocaldarius*.[1a,c,6] These remarkable studies have been performed mainly by the groups of Wu, Matsuda, and Ebizuka, as well as our group. We have previously reported the detailed kinetics of the reactions of site-directed mutants of the prokaryotic hopene cyclase (SHC),[1a,6c,e,f,i–k] and thus we could propose with high credibility the function of the active sites, based on both the considerable kinetic data estimated (K_m and k_{cat}) and the product distributions. However, the enzyme activity of the mutated OSCs relative to that of the wild-type enzyme, regardless of in vivo or in vitro experiments, has rarely been reported to date,[3–5] and

[a] R. Ito, I. Hashimoto, Y. Masukawa, Prof. Dr. T. Hoshino
Graduate School of Science and Technology
Niigata University, Ikarashi 2-8050
Nishi-ku, Niigata 950-2181 (Japan)
E-mail: hoshitsu@agr.niigata-u.ac.jp

[b] Prof. Dr. T. Hoshino
Department of Applied Biological Chemistry
Faculty of Agriculture, Niigata University, Ikarashi 2-8050
Nishi-ku, Niigata 950-2181 (Japan)

Supporting information for this article is available on the WWW under http://dx.doi.org/10.1002/chem.201301917. It contains a number of additional figures and the spectroscopic data the compounds synthesized.

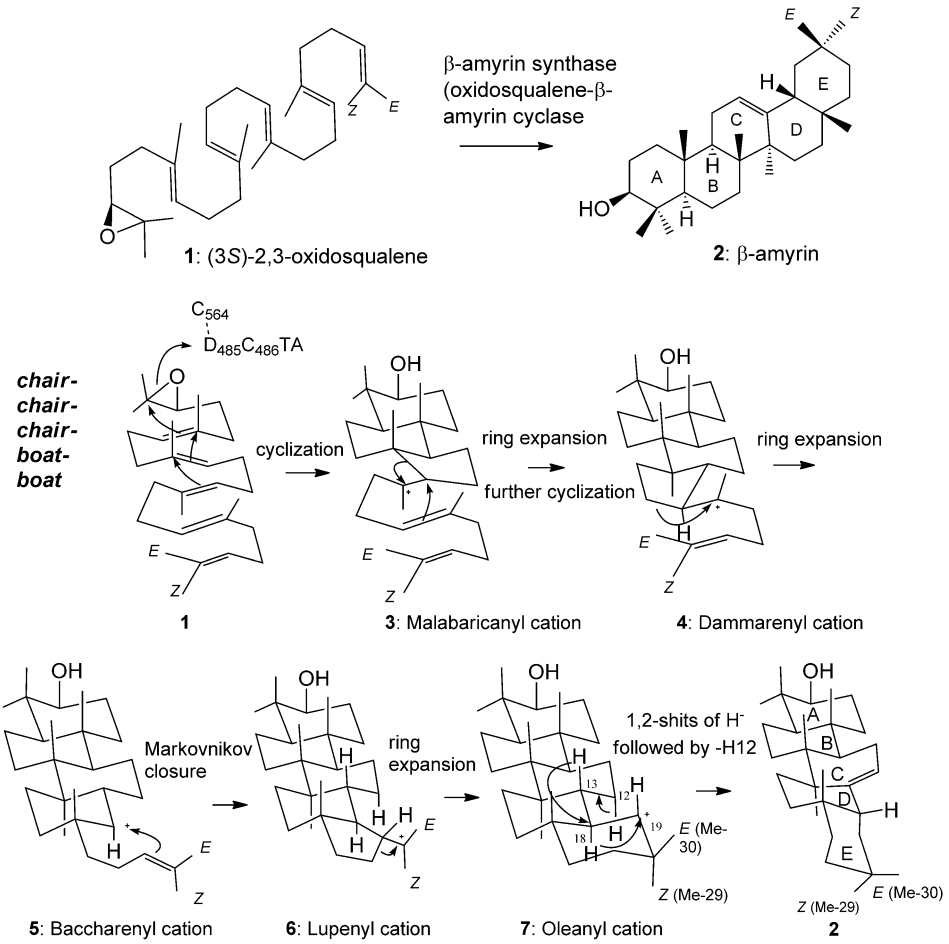

Scheme 1. Biosynthetic mechanism for the formation of β-amyrin (**2**) from (3*S*)-2,3-oxidosqualene (**1**). The substrate **1** is folded in a chair–chair–chair–boat–boat conformation in the enzyme cavity, and the proton released from the DCTA amino acid motif attacks the epoxide ring, leading to the sequential ring-forming reactions and the construction of the 6,6,6,6,6-fused pentacyclic ring scaffold **7** via carbocationic intermediates **3**, **4**, **5**, and **6**. The oleanyl cation **7** undergoes the rearrangement reactions of 1,2-hydride shifts and loss of the axial-oriented H12 to yield β-amyrin **2**.

the function of the amino acids conserved among OSCs have been discussed mainly in light of the product distributions. Thus, the exact functions of the active-site residues are yet to be addressed.

β-Amyrin is widely found in the plant kingdom and constitutes the fundamental scaffold of glycyrrhizin, which is a major bioactive compound derived in the underground parts of *Glycyrrhiza* (licorice) plants, possesses a wide range of pharmacological properties, and is used worldwide as a natural sweetener. β-Amyrin is biosynthesized by folding (3*S*)-2,3-oxidosqualene in a chair–chair–chair–boat–boat conformation inside the OSC cavity (Scheme 1). This conformation was proposed in 1955 by Eschenmoser et al.[7] The folded conformation imposed by β-amyrin cyclase undergoes the cyclization reactions through epoxide ring opening to yield a malabaricanyl cation **3** with a 6,6,5-fused tricyclic ring system, which is subjected to ring expansion and further cyclization to produce a dammarenyl cation **4** with a 6,6,6,5-fused tetracycle. Next, the second enlargement from a 5- to a 6-membered ring affords the baccharenyl cation **5** with a 6,6,6,6-fused tetracycle, and further cyclization gives the 6,6,6,6,5-fused pentacyclic lupenyl cation **6**, which subsequently undergoes a third ring-expansion process to give the final oleanyl cation **7** with a 6,6,6,6,6-fused pentacyclic structure. The antiparallel-fashion hydride shifts of H13 to C18 and H18 to C19, followed by loss of H12, finally furnish β-amyrin.

Mutational studies on β-amyrin cyclase are very limited; only one study has been published on the mutational experiments for the Tyr261 and W259 groups of β-amyrin synthase from *Panax ginseng* (PNY1).[8] However, the enzyme activity of these mutants relative to that of the wild type has not yet been estimated, and furthermore, the functional analyses of any other residues conserved in β-amyrin cyclases have not been reported. Recently, we succeeded in obtaining high-level expression of β-amyrin synthase from *Euphorbia tirucalli* (EtAS) in *S. cerevisiae* GIL77, lacking the ERG7 gene (lanosterol synthase) and in estimating the enzyme activity of the site-directed mutants.[9a] We found that the Asp group in the $D^{485}C^{486}$TA motif, highly conserved in OSCs, triggers the initiation of the polycyclization reaction and that C564 is involved in hydrogen-bond formation with the carboxyl residue of D485, resulting in enhancement of the acidity.[9a]

In this study, we assess the in vivo enzymatic activities of the site-directed mutants targeted to the Phe728 residue of EtAS, which is highly conserved in the OSC and SHC families (see the Supporting Information, Figure S1); the protein levels of the EtAS variants expressed in the yeast lacking lanosterol synthase were quantified by western blot analysis and the amounts and distribution of triterpene products, generated by the range of variants, were determined by gas chromatography (GC). The experimental results provide unambiguous evidence that the Phe728 residue is located in the D/E-ring-formation site and stabilizes the tetra- and pentacyclic cations, **4**, **5**, **6**, and **7**, leading to the efficient formation of the β-amyrin scaffold through cation–π interactions. In addition, the steric size at this position plays a key role in directing the polycyclization pathway and also affects

the enzyme activity, possibly due to the altered binding of substrate **1** with the mutated EtASs.

Results and Discussion

Identification of triterpene products generated by the site-specific mutants: Six site-directed variants were constructed by substituting Phe728 (F728) with Ala, Ile, Met, His, Tyr, or Trp. Mutagenesis of F728 in the wild-type pYES2-EtAS/CT, constructed earlier by our group,[9a] was performed by using the QuikChange site-directed-mutagenesis method. The products were monitored by GC (see the Supporting Information, Figure S2). The F728H and F728W mutants afforded many products. Large-scale cultures (50 L) of each mutant enabled the isolation of the triterpenes produced by the mutants. The yeast cells of the His mutant were suspended in 15% KOH/MeOH (1 L) and heated to reflux three times, followed by extraction of the lipophilic materials with *n*-hexane (9×1 L). The cyclic-triterpene-rich fraction was obtained by partial purification with a SiO_2 column to remove oxidosqualene (**1**), dioxidosqualene, and nontriterpene impurities by using a hexane/EtOAc (100:1) mixture as the eluent. The triterpene-containing fraction (ca. 198 mg) was acetylated with Ac_2O/pyridine (py) and further purified with a SiO_2 column with hexane/EtOAc (100:0–0.6) to completely remove the remaining dioxidosqualene. Figure 1 shows the GC profile of the acetate fraction from the His mutant. Products **8**–**20** were numbered in order of elution from GC analyses (Figures 1 and 2).

The acetylated fraction was subjected to repeated HPLC steps (isocratic elution, hexane/THF, 100:0.15 and 100:0.07),

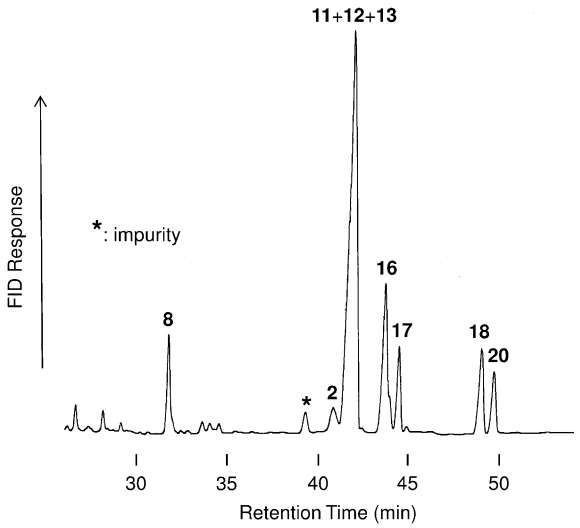

Figure 1. GC trace of triterpene acetates produced by the F728H mutant. The triterpene fraction was obtained by partial purification with a SiO_2 column to remove oxidosqualene, dioxidosqualene, and nontriterpene impurities (hexane/EtOAc, 100:1), followed by acetylation with Ac_2O/py. The acetate mixture was subjected to GC analysis. GC conditions were as follows: J&W, DB-1 capillary column (length 30 m, internal diameter 0.32 mm, film thickness 0.25 μm); injection *T* 300°C; column *T* 190–250°C (10°C min^{-1}), 250–260°C (0.35°C min^{-1}).

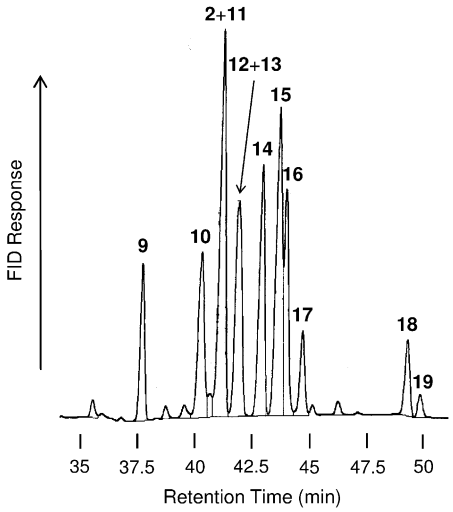

Figure 2. GC profile of triterpene acetates obtained by the F728W mutant. The triterpene fraction was obtained by the partial purification with a SiO_2 column to remove oxidosqualene, dioxidosqualene and non-triterpene impurities (hexane/EtOAc, 100:5), followed by acetylation with Ac_2O/py. The acetate mixture was subjected to GC analysis. GC conditions were the same as those described for Figure 1.

giving pure acetates of nine products (i.e., **2**, **8**, **11**–**13**, **16**–**18**, and **20**). The acetates of products **12** and **17** were separated by using a chiral column (Daicel Chiral Pak IB). The structures of all of the products were determined by detailed NMR analysis, including DEPT, ^{1}H–^{1}H COSY, HOHAHA, NOESY, HMQC (or HSQC), and HMBC spectroscopy (see the Supporting Information, Figure S3).

The structure of **11**Ac was determined as follows: The six vinylic methyl groups of **1** (δ_H = 1.68–1.60 ppm) disappeared, while eight new aliphatic methyl groups appeared (δ_H = 1.01–0.72 ppm, each 3H, s) in the ^{1}H NMR spectrum ($CDCl_3$, 600 MHz), suggesting that **1** was fully cyclized to afford a pentacyclic product. Clear HMBC cross-peaks were observed between the olefinic proton (H19, δ_H = 4.86 ppm, 1H, s) and the following carbon atoms: C13 (δ_C = 38.38 ppm, d), C17 (34.33, s), C18 (142.7, s), C20 (32.35, s), C21 (33.32, t), and C29 and C30 (29.17, q and 31.33 ppm, q). This finding suggested that compound **11** was germanicol, the stereochemistry of which was confirmed by the NOESY spectrum. All of the other NMR data were consistent with the proposed germanicol structure. The position of the double bond was the only difference between compounds **11** and **2** (see the structures given in Scheme 2). Detailed analyses of the NMR data are shown in the Supporting Information, Figure S3.4.

The chemical structure of product **20** was determined as follows: Three olefinic Me groups were found at δ_H = 1.67 ppm (Me26, 3H, s), 1.69 (Me21, 3H, brs), and 1.60 ppm (Me27, 3H, s). The proton signals of both Me26 and Me27 correlated with both C25 (δ_C = 131.2 ppm, s) and C24 (124.6 ppm, d) in the HMBC spectrum. Furthermore, Me21 (δ_H = 1.69 ppm, 3H, brs) and H22 (1.88, 1H, m; 1.99 ppm, 1H, m) also generated strong HMBC cross-peaks with C20 (δ_C = 125.9 ppm, s) and C17 (136.4 ppm, s). These

data clarified the position of the double bonds (C24=C25 and C17=C20). The unambiguous NOEs between Me21 and H12 ($\delta_H = 2.27$ ppm, 1H, d, $J = 15.8$ Hz) and between H22 (1.88, m; 1.99, m, each 1H) and H16 (2.22 ppm, 1H, m) indicated the presence of the *E* isomer of the double bond. A strong NOE between H5 ($\delta_H = 0.83$ ppm, 1H, m) and H9 (1.37 ppm, 1H, m) indicated an α-orientation of H9. Thus, the structure of **20** was assigned as (17*E*)-dammara-17(20),24-diene-3β-ol. The analogous compound, (17*Z*)-protosta-17(20),24-diene-3β-ol (protostadienol), was found to be the biosynthetic precursor of helvolic acid (fusidane class),[5b,10] which shows antibiotic activity. The structural differences between protostadienol and **20** are as follows: 9β-H for protostadienol and 9α-H for **20**; and the *Z* isomer for protostadienol, but *E* geometry for **20** at the C17=C20 double bond. Compound **20** is an unnatural natural product that, to our knowledge, has not been reported before.

Product **13**, (20*E*)-dammara-20(22),24-dien-3β-ol, was also isolated from the Y261H variant of PNY β-amyrin synthase together with **10**[8] (see the Supporting Information, Figure S1, for the amino acid alignment). The structures of products **2**, **8**, **12**, **13**, and **16**–**18** were determined by detailed NMR analysis (see the Supporting Information, Figure S3). We have previously isolated products **10**, **12**, **15**, and **17** as the enzymatic products of *Oryza sativa* triterpene cyclases.[9b] Comparison of the MS and NMR spectra of these compounds with those of the *Oryza sativa* triterpenes confirmed these assignments. In case of the His mutant, the production of **2** significantly decreased (3%), whereas the lupane skeleton **16** (lupeol, 15%) and taraxasteryl core **18** (ψ-taraxasterol, 8%) were generated as pentacyclic products in addition to the oleanyl scaffold **11** (51%). Furthermore, a substantial amount (17.3%) of tetracyclic products from dammarenyl cation **4** was found. The 6,6,5-fused tricyclic structure of malabaricane skeleton **8** was obtained in 5.6% yield. The product distribution ratio is shown in Table 1.

As shown in Figure 2, the Phe728Trp variant also afforded many cyclic triterpenes. The following 12 triterpenes were detected as enzymatic products: **2**, **9**, and **10**–**19**. Pure triterpenes were isolated by employing a SiO_2 and a chiral column for HPLC in a similar manner as for the F728H mutant.

The structure of product **14**, which was specifically produced by F728W, was determined as follows: ^{1}H NMR analysis (600 MHz, [D$_6$]acetone) showed eight methyl signals resonating at high field ($\delta_H = 1.08$–0.844 ppm), suggesting that the molecule did not contain olefinic methyl groups; therefore, a pentacyclic skeleton was assigned to **14**. Either ursanyl or taraxasteryl skeletons were assignable because 2Me doublet signals and 6Me singlet signals were found: $\delta_H = 1.03$ ppm (Me29, 3H, d, $J = 7.0$ Hz) and 0.977 ppm (Me30, 3H, d, $J = 6.8$ Hz) for the 2Me doublets. Me26 ($\delta_H =$ 1.08 ppm, 3H, s) and Me27 (0.968 ppm, 3H, s) had a clear HMBC correlation with C14 ($\delta_C = 160.2$ ppm, s). Furthermore, H15 ($\delta_H = 5.52$ ppm, dd, $J = 7.7$, 2.5 Hz) had definitive HMBC cross-peaks with C13 (40.81 ppm, s) and C14. Thus, a double bond is positioned at C14–C15. The strong NOEs of Me26/Me28 ($\delta_H = 0.933$ ppm, 3H, s) and Me27/H16 ($\delta_H =$ 2.08 ppm, m) and the absence of an NOE for Me26/Me27 indicated that Me27 and Me28 were arranged in α- and β-orientations, respectively. A strong NOE for Me29/H18 ($\delta_H = 0.93$ ppm, m) and for Me29/H12 (1.56 ppm, m), in addition to the lack of NOE for Me28/Me30, verified the assignment of the β-configuration for Me29 and the α-arrangement for Me30 (see the Supporting Information, Figure S3.7). These configurations are further supported from the biogenetic point of view, as described below. Thus, as shown in Scheme 2, product **14** was determined to be isoursenol, a triterpene that has rarely been found in nature and was first isolated from the leaves of *Olearia paniculata*.[11] In addition, **14** has not been previously reported in the many mutagenesis experiments on OSCs.[3–5] The structures of the other triterpenes **8**–**20** (Scheme 2) were determined by detailed 2D NMR analysis (Supporting Information, Figures S3.1–S3.13).

The polycyclization pathway of 1 to form products 8–20: Scheme 2 shows the polycyclization pathway of **1** to give products **8**–**20**. As shown in Scheme 1, substrate **1** was folded in a chair–chair–chair conformation to produce the malabaricanyl cation **3**, followed by the deprotonation of Me27, affording **8** (malabaricatritene). Cation **3** was also subjected to further cyclization through two routes: 1) an unusual chair–chair–chair–chair folding conformation to yield the 17-*epi*-dammarenyl cation **4′** and 2) the normal chair–chair–chair–boat folding to give dammarenyl cation **4**. The two cations, **4′** and **4**, underwent 1,2-migration reactions of a hydride and the methyl group (H17α,β→C20, H13β→C17, Me30α→C13, Me18β→C14), followed by loss of H7, yielding **17** and **12**, respectively. In our previous paper, we reported that negligible amounts of **17** and **12** are produced by the wild-type enzyme.[9a] The 6,6,6,5-fused tetracyclic cation **4** also underwent ring expansion, leading to the 6,6,6,6-fused baccharenyl cation **5**. Further cyclization gave the 6,6,6,6,5-fused pentacyclic lupenyl cation **6**, which underwent the 1,2-shift of three hydride ions (H19β→C20, H18α→C19, and H13β→C18) in an antiperiplanar manner and the loss of H12, leading to the formation of **9**. Proton elimination from Me29 in cation **6** gave lupeol **16**. A further expansion process from the 5-membered E ring of **6** to the 6-membered E ring generated the 6,6,6,6,6-fused pentacyclic oleanyl cation **7**. Loss of H18α gave **11**. Shifts of H18α to C19 and H13β to C18 in an antiparallel manner, followed by loss of H12α, gave β-amyrin **2** (see also Scheme 1). The substitution of Phe with His or Trp at the 728-position of the enzyme induced the shunt pathway, which led to the production of the taraxasteryl (**21**) and ursanyl (**22**) cations, which have not been detected for the aliphatic or Tyr mutants, or for the wild-type enzyme (Phe). Me29α (terminal (*Z*)-Me shown in Scheme 1) of cation **7** shifted to C19, yielding cation **21**, which underwent further hydride shifts in an antiperiplanar manner (H19β→C20, H18α→C19, H13β→C18), affording cation **22**. The proton-elimination reactions of H21 and Me30 from cation **21** gave **18** and **19**, respectively.

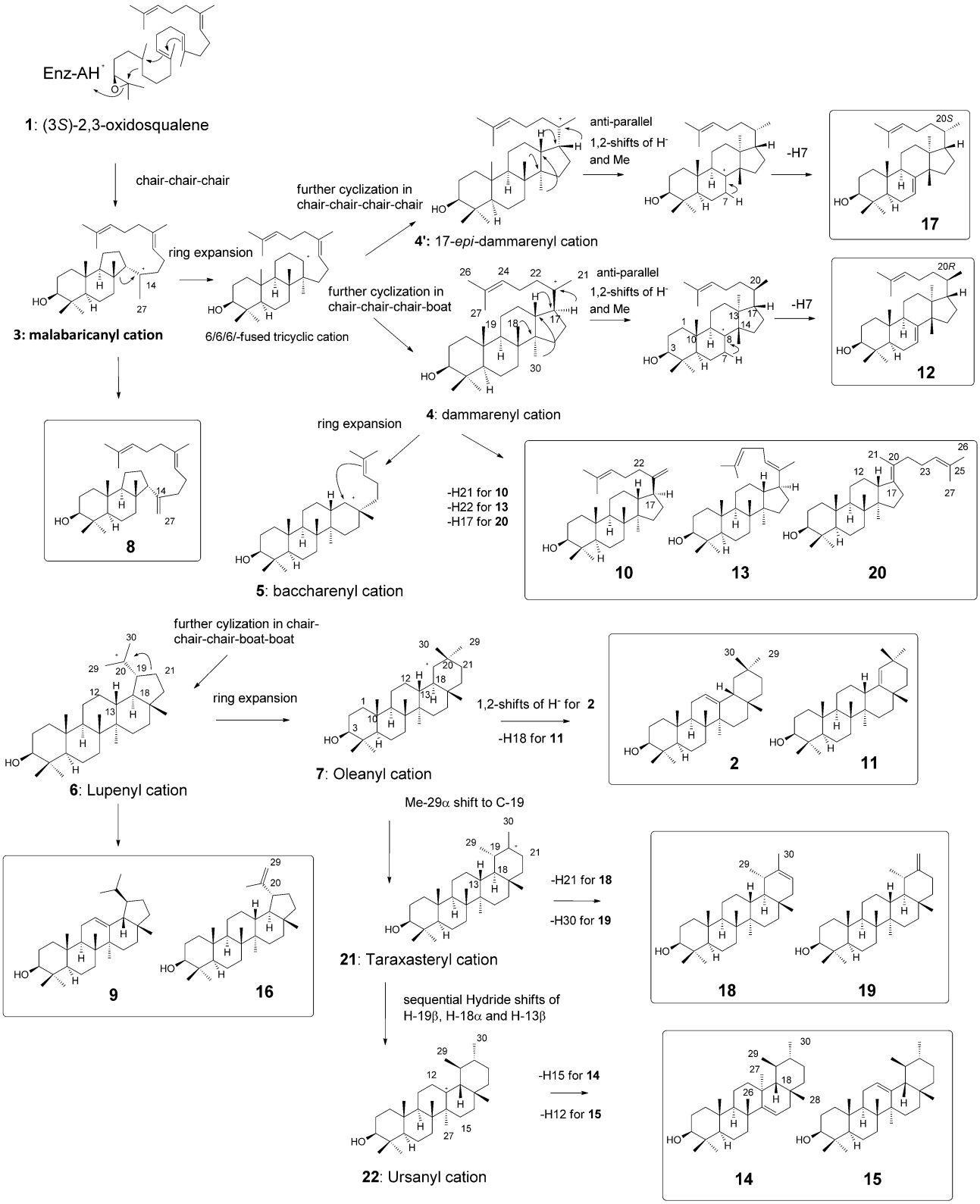

Scheme 2. The proposed biosynthetic pathway for the formation of the cyclic triterpenes obtained in this study. Products **8**–**20** were numbered in order of elution from the GC analyses (Figures 1 and 2). Product names: **8** = (17*E*)-(13β*H*)-malabarica-14(27),17,21-trien-3β-ol, **9** = lup-12-en-3β-ol, **10** = dammara-20(21),24-dien-3β-ol, **11** = germanicol, **12** = butyrospermol, **13** = (20*E*)-dammara-20(22),24-dien-3β-ol, **14** = isoursenol, **15** = α-amyrin, **16** = lupeol (lup-20(29)-3β-ol), **17** = tirucalla-7,24-dien-3β-ol, **18** = ψ-taraxasterol (urs-20(21)-en-3β-ol), **19** = taraxasterol (urs-20(30)-en-3β-ol), **20** = (17*E*)-dammara-17(20),24-dien-3β-ol (a novel compound).

The Me shift (Me27α→C13) and loss of H15 on cation **22** could provide product **14**. The elimination of H12 of cation **22** could give **15**.

The Ala and Met variants never generated cations **21** and **22** and nor did the Phe and Tyr mutants, but the His and Trp mutants did yield these cations. This finding suggests that not only the appropriate steric bulk, but also the π-electron system of the aromatic ring are required at this position to avoid divergent pathways. His and Trp, as well as Phe and Tyr, have a π-electron system, but the side chain sizes of His and Trp are smaller and larger, respectively, than those of Phe and Tyr. Furthermore, a question arises regarding why only Trp mutant afforded cation **22**. The Trp residue possesses the largest steric volume among the side chains, leading to significantly lowered activity due to looser binding, but its rich π-electron configuration could still facilitate the formation of cation **22** through cation–π interactions, as discussed below (Figure 3).

Enzyme activities of the mutants relative to that of the wild-type enzyme: The expressed amounts of mutated OSCs are frequently found to be none or significantly decreased. However, no report describing the OSC expression level of the mutants has been published.[3–5] For in vivo analysis of the function of the site-directed variants, it is crucial to determine both the amount of the expressed OSC enzymes and the quantities of the triterpenes produced by the mutants, and then the relative activities must be compared against that of the wild-type enzyme. The enzyme activities are determined by dividing the amount of the product produced in vivo by the amount of EtAS protein expressed in the mutants and the wild-type. We used our recently developed protocol[9] to estimate the amount of protein by western blot analysis (see the Supporting Information, Figure S4), and the quantities of β-amyrin or all of the triterpenes produced were determined by GC (see the Supporting Information, Figure S5). As seen in the Supporting Information, Figure S4, the expression levels of EtAS varied depending on the variant. No expression of the Val and Leu mutants was observed by the western blot method, although the codons were changed by using different primers for QuikChange. The expression level of F728I EtAS was negligibly small (see the Supporting Information, Figure S4). Next, we constructed the Met variant, which showed a high expression level (Figure S4). Figure 3 shows the relative activities estimated by in vivo experiments. The Tyr mutant had nearly the same activity as the wild type, but the Ala and Met mutants had significantly deceased activities. We have provided strong evidence to show that the interaction between the π-electrons of the aromatic amino acid residues and the transient carbocation intermediate generated during the polycyclization reaction of squalene (cation–π interaction) gives an efficient cyclization reaction.[6c] The decreased activities of the Ala and Met mutants would be accounted for by the lack of π-electrons in the side chains. The Met variant had a somewhat higher activity than the Ala variant. This may be due to the fact that the size of Met is nearly equivalent to that of Phe, which could result in an almost similar product distribution as that for the wild-type enzyme (Table 1). It has been indicated that the steric bulk influences the activity, as well as the cyclization pathway that directs what kind of products are produced.[1a,3–6] It is questionable whether the His variant had a significantly lower activity despite the imidazole ring having π-electrons. The imidazole ring may be partly protonated, in which case the cation–π interaction does not occur, but it might still exist in the free form (the not protonated form) inside the reaction cavity, which could eliminate the H18 atom of the oleanyl cation to yield germanicol **11** as the main product. The partly protonated His residue may have led to the considerably reduced enzyme activity. Mecozzi et al. reported the cation–π-electron binding energies of the aromatic rings with Na^+ as follows: 21.0 for His, 27.1 for Phe, 26.9 for Tyr, and 32.6 kcal mol^{-1} for Trp.[12] Thus, it is envisaged that the Trp mutant should have the highest activity because it has the highest binding energy of the indole ring compared to those of Phe, Tyr, and His; however, its activity was significantly decreased and almost equivalent to that of the Ala variant. This could have occurred due to the significantly decreased binding of **1** with the active site, which was caused by embedding the larger steric bulk of Trp in the site. The activities of F365W and F605W mutants of the SHC enzyme were also markedly decreased,[6i,j] as observed with the F728W mutant of this β-amyrin synthase. Currently, it is inferred that the enzyme activity is affected not only by cation–π electron interactions, but also by the steric bulk of the active-site residues.[6] To verify this idea, we tried to estimate the K_m and k_{cat} values of the purified EtAS variants, but failed due to the extremely decreased activities in the in

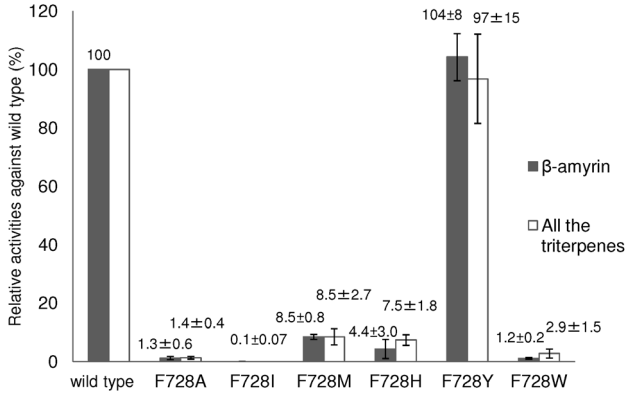

Figure 3. Relative activities of the site-directed mutants with respect to that of the wild-type enzyme. These relative activities were estimated by dividing the quantity of β-amyrin or all of the triterpenes produced by the amount of expressed EtAS protein. The quantities of β-amyrin and all of the triterpenes produced were determined by GC analysis using geranylgeraniol as the internal standard. The amounts of the expressed EtAS were quantified by use of a western blot method. The activities of the wild-type EtAS for the formation of β-amyrin and all of the triterpene products were 5.02±0.79 and 5.62±0.17 (mg of the produced triterpene per mg of the expressed protein), respectively. In the case of the His mutant, the quantity of β-amyrin was calculated as the sum of germanicol **11** and β-amyrin **2** produced because the two triterpenes are produced from an identical intermediate, the oleanyl cation **7**.

vitro experiments (see the specific activities of the purified EtAS variants in the Supporting Information, Figure S6.1). Although the Triton X-100 used in the in vitro assay[9] was replaced by other detergents, such as *n*-dodecyl-β-D-maltoside or IGEPAL CA-630, the in vitro activity did not improve. The CD spectra of the purified EtAS mutants were almost the same as that of the wild type (see the Supporting Information, Figure S6.2), suggesting that the alteration of the protein architecture caused by these mutations was negligible. It is not clear why the activity significantly decreased in the in vitro assay, including that for the Tyr mutant. However, only the Tyr mutant exhibited a relatively high specific activity compared with other mutants (see the Supporting Information, Figure S6.1); this result was consistent with those of the in vivo assays (Figure 3). Thus, it could be assumed that the main role of Phe728 is to stabilize the intermediate through cation–π interactions and that the steric bulk of Phe is most appropriate; Tyr is not large enough to change the binding of **1** with this OSC, but Trp is too large to acquire the tight binding, leading to the lowered activity and to interruption of the polycyclization cascade at the intermediate stages, as described below.

Insights into the product distribution of triterpenes generated by the site-specific mutants: Table 1 summarizes the distribution (%) of the products generated by each of the mutants. The high ratio of **11** and formation of product **11** are specific to the His mutant, clearly indicating that the Phe728 residue is localized in the proximity of the D/E-ring-formation site inside the reaction cavity (see the homology modeling in the Supporting Information, Figure S7). The basic His residue substituted at position 728 behaved as a proton acceptor, as described above. However, the Trp moiety does not exert a basic functionality, resulting in no production of **11** and **20**. In turn, despite the markedly decreased activity (Figure 3), the Trp mutant promoted the formation of ursanyl cation **22** (C13 cation) through a cation–π interaction, leading to the production of α-amyrin **15** and isoursenol **14**. However, the wild type (Phe) and the Tyr mutant enzymes showed no production of cation **22** and almost exclusively afforded the oleanyl C19 cation **7**, suggesting that the Phe728 moiety is located next to C19 and stabilizes the secondary cation **7**. The Phe in the wild-type enzyme or the Tyr in the mutant could not stabilize the C13 cation of **22**, because the π-electron frame is less extended due to the smaller size compared with that of Trp. In addition, the Trp variant showed a significantly higher distribution of tetracyclic products (27.3%) than the wild type (3.4%) and the Tyr mutant (4.4%), clearly indicating that the steric bulk guided the polycyclization pathway. The larger size of Trp could have caused the looser binding of the substrate with the D/E-formation site inside the reaction cavity, so that the polycyclization stopped at a premature stage, furnishing higher product ratios of the tetracyclic products **10**, **12**, **13**, and **17**. The imidazole ring of His has a bifunctional role, both abstracting a proton as a base and stabilizing the intermediate cations through a cation–π interaction. The formation of **18** via the taraxasteryl cation **21** may have resulted from the two functions of the His moiety, that is, the stabilization of the C20 cation of cation **21** and removal of H21. This mutant also afforded a relatively higher yield of lupeol **16** (15%) than the Trp mutant (9%). This finding further indicates the basic function of the His moiety in eliminating H29 of the lupenyl cation **6**. However, the cation–π binding energy of the His residue is the most modest amongst the other aromatic rings;[12] therefore, the His residue could not sufficiently stabilize the secondary baccharenyl cation **5**, leading to a high ratio of the tertiary dammarenyl cation **4**. As described above, the cation-binding energy of His may have been further decreased, in part due to the formation of the protonated imidazole ring. We have reported definitive evidence that both the cation–π interaction and the steric bulk direct the polycyclization pathway of squalene by hopene cyclase.[1a,6c] The Ala mutant could not stabilize the intermediate cation **5** owing to the lack of π-electrons; thus, increased production of cation **4** (39%) was accompanied by the decreased ratio of cation **7** (52%). The smaller size of the Ala residue could further increase the proportion of cation **4** formed due to the poor interaction with the active-site residues. The Ala variant produced **17** in a significantly higher ratio (34%) than the other mutants. In the case of the formation of **17**, **1** was folded in an unusual chair–chair–

Table 1. Distribution ratio of the products [%] generated by each of the mutants. Each of the values represents the percentage of the triterpene produced.[a]

	Tricycle from **3**	Tetracycle from **4**						Pentacycle from **6** (lupenyl cation)			Pentacycle from **7** (oleanyl cation)			Pentacycle from **21** and **22** (taraxasteryl and ursanyl cations)					
Product	**8**	**10**	**12**	**13**	**17**	**20**	Total	**9**	**16**	Total	**2**	**11**	Total	**14**	**15**	**18**	**19**	Total	Unidentified products
wild type	–	–	1.8	–	1.6	–	3.4	–	–	–	96.6	–	96.6	–	–	–	–	–	0
F728A	–	–	5.3	–	**34.0**[b]	–	**39.3**[b]	–	5.6	5.6	52.0	–	52.0	–	–	–	–	–	3.1
F728I	–	–	–	–	-	–	–	–	–	–	–	–	–	–	–	–	–	–	–
F728M	–	–	4.7	–	11.3	–	16.0	–	–	–	72.9	7.4	80.3	–	–	–	–	–	3.7
F728H	5.6	–	1.8	3.4	6.1	**6.0**[b]	17.3	–	**15.1**[b]	15.1	3.2	**50.9**[b]	54.1	–	–	**7.9**[b]	–	7.9	0
F728Y	–	–	1.1	–	3.3	–	4.4	–	–	–	95.6	–	95.6	–	–	–	–	–	0
F728W	–	9.8	11.9	1.9	4.0	–	**27.3**[b]	6.7	9.1	15.8	17.2	3.3	20.5	**13.2**[b]	**18.0**[b]	3.8	1.1	36.1	0.3

[a] Products **8**–**20** were numbered in order of elution from the GC analyses (Figures 1 and 2). [b] Bold values highlight the functional features of each of the mutants.

chair–chair conformation, which differs from the normal chair–chair–chair–boat conformation, leading to the formation of **12** (5.3%). The Met mutant was constructed to inspect the effect of the steric bulk; whereas Ala is too small, the bulk of Met is nearly equivalent to that of Phe. The product distribution for the Met mutant is shown in Table 1. A high proportion of cation **4** (16%) was also observed, as seen in the Ala variant. In addition, the proportion of **17** formed by the Met mutant (11%) was lower than that by the Ala variant (34%), strongly supporting the idea that the steric bulk directs the stereochemical destiny of the products; this has also been demonstrated in the case of the SHC enzyme.[6f,h] The product distribution of the Tyr variant was the same as that of the wild-type enzyme. The Tyr residue has almost the same cation–π binding energy and nearly the same steric bulk as the wild-type (Phe) residue; this feature could account for the same product distribution and formation of the same products as the wild-type enzyme, as shown in Table 1.

Conclusion

The concept of cation–π interactions for the cationic squalene cyclization was first proposed by Dougherty.[13] As mentioned above, the steric bulk directs the enzyme activity, as well as the polycyclization pathway. Thus, differences in the steric bulk of the catalytic sites must be avoided to verify presence of the cation–π interaction. We site-specifically incorporated unnatural fluorophenylalanine instead of Phe into the catalytic site of SHC; a fluorine atom has an extremely high electronegativity, but a similar van der Waals radius to that of hydrogen. The activity of the SHC variants with fluorophenylalanine were found to be inversely proportional to the number of fluorine atoms on the aromatic ring and clearly correlated with the cation–π binding energies of the ring moiety.[6c] To our knowledge, this study is the first to provide unambiguous evidence for cation–π interactions during the catalytic action of SHC. Recently, the significance of the cation–π interaction was also pointed out for sesquiterpene synthase.[14] The enzymatic activity of the mutants must be determined to propose the cation–π interaction as the catalytic action by OSCs, but few studies have been performed on this activity. By employing western blot and GC techniques, we developed a simple method for estimating the in vivo activities of the mutated OSCs (Figure 3). The Tyr variant showed nearly the same activity as the wild-type (Phe) enzyme. This could have been caused by the small difference in the steric bulk and the cation–π binding energies of Phe and Tyr. The main product of the His mutant was germanicol (**11**), supporting the hypothesis that F728 is located in the proximity of the D/E-ring-formation site. The steric bulk also guided the polycyclization pathway and the folding conformation determining the stereochemical destiny of the products. Variations in the steric bulk (smaller or larger volume) are considered responsible for the different proportions of the intermediate cations, **3**, **4**, **5**, **6**, and **7**, formed, which then underwent the 1,2-shifts of hydride and methyl groups to quench the cations, resulting in the formation of a variety of prematurely cyclized products (Scheme 2). The introduction of other amino acids with different steric bulks could further have given rise to local changes surrounding the active site in the protein architecture. In conclusion, the major function of Phe728 is to stabilize the carbocation intermediates **4**, **5**, **6**, and **7**. In particular, the stabilization of the secondary cations **5** and **7** by Phe728 could facilitate the ring expansion processes **4**→**5** and **6**→**7**. The position of the Phe728 residue in the reaction cavity would move during the process **4**→**5**→**6**→**7** to orient the benzene ring optimally for stabilizing each carbocation. This is the first report to experimentally demonstrate that cation–π interactions play a crucial role for the catalytic action of OSCs. Furthermore, through this investigation, we succeeded in creating the unnatural product **20** and the triterpene scaffold isoursenol **14**, which is rarely found in nature.

Experimental Section

Instruments: NMR spectra were recorded in $CDCl_3$ or C_6D_6 with a Bruker DMX 600 or DPX400 spectrometer. The chemical shifts (δ) are given in ppm relative to the residual solvent peak as the internal reference ($\delta_H = 7.26$ and $\delta_C = 77.0$ ppm for $CDCl_3$; $\delta_H = 7.28$ and $\delta_C = 128.0$ ppm for C_6D_6; $\delta_H = 2.04$ and $\delta_C = 29.80$ ppm for [D_6]acetone). GC analyses were performed on a Shimadzu GC-2014 chromatograph fitted with a flame ionization detector (J&W DB-1 capillary column, 0.25 mm × 30 m). GC/MS spectra were obtained with a JMS-Q1000 GC K9 (JEOL) instrument under electronic impact at 70 eV with a Zebron ZB-5 ms capillary column (0.25 mm × 30 m), the oven temperature being elevated from 220 to 270 °C (3 °C min^{-1}).

Mutagenesis experiments: Mutagenesis of Phe728 in wild-type pYES2-EtAS/CT was performed with the QuikChange site-directed mutagenesis method. The following oligonucleotide primers were used; substitutions are underlined.

For the F728A variant: The sense primer was 5′-GATAACGGGTGTGGCCATGAAGAATTGCATG-3′ and the antisense primer was 5′-CATGCAATTCTTCATGGCCACACCCGTTATC-3′.

For the F728H variant: The sense primer was 5′-CAGCAGGAGATAACGGGTGTGCACATGAAG-3′ and the antisense primer was 5′-CTTCATGTGCACACCCGTTATCTCCTGCTG-3′.

For the F728I variant: The sense primer was 5′-GCAGGAGATAACGGGTGTGATCATGAAGAATTGCATG-3′ and the antisense primer was 5′-CATGCAATTCTTCATGATCACACCCGTTATCTCCTGC-3′.

For the F728M variant: The sense primer was 5′-CAGCAGGAGATAACGGGTGTGATGATGAAGAATTGCATG-3′ and the antisense primer was 5′-CATGCAATTCTTCATCATCACACCCGTTATCTCCTGCTG-3′.

For the F728W variant: The sense primer was 5′-GATAACGGGTGTGTGGATGAAGAATTGCATG-3′ and the antisense primer was 5′-CATGCAATTCTTCATCCACACACCCGTTATC-3′.

For the F728Y variant: The sense primer was 5′-CAGCAGGAGATAACGGGTGTGTATATGAAG-3′ and the antisense primer was 5′-CTTCATATACACACCCGTTATCTCCTGCTG-3′.

For the F728V variant: The sense primer was 5′-GATAACGGGTGTGGTCATGAAGAATTGCATG-3′ and the antisense primer was 5′-CATGCAATTCTTCATGACCACACCCGTTATC-3′.

For the F728L variant: The sense primer was 5′-GGAGATAACGGGTGTGTTGATGAAGAATTGC-3′ and the antisense primer was 5′-GCAATTCTTCATCAACACACCCGTTATCTCC-3′.

PCRs were conducted with a 16-cycle program: 98°C for 0.5 min, 60°C for 1 min, 68°C for 9 min, and a final extension at 68°C for 9 min. KOD-plus DNA polymerase (Toyobo) was used with dNTPs (0.2 mM), dimethylsulfoxide (5%) and $MgSO_4$ (0.1 mM) in a final volume of 50 μL. Mutations were confirmed by DNA sequencing with the dideoxy chain-termination method and a Beckman Coulter CEQ8000 (Beckman Coulter).

Measurements of in vivo protein expression levels and CD measurement: These experimental protocols were described in a previous paper.[9a]

Data for 14: $[\alpha]_D^{25} = -29.8$ ($c = 0.094$ in $CHCl_3$); there is no literature data for the $[\alpha]_D$ of **14**; solid; ^{1}H NMR (600 MHz, [D$_6$]acetone): $\delta = 0.844$ (s, 3H; Me23), 0.872 (s, 3H; Me24), 0.90 (dd, $J = 12.5$, 2.7 Hz; H5), 0.93 (m, 1H; H18), 0.933 (s, 3H; Me28), 0.964 (s, 3H; Me25), 0.968 (s, 3H; Me27), 0.977 (d, $J = 6.8$ Hz, 3H; Me30), 1.030 (m, 1H; H1), 1.030 (d, $J = 7.0$ Hz, 3H; Me29), 1.079 (s, 3H; Me26), 1.29 (m, 2H; H20, H22), 1.33 (m, 1H; H7), 1.35 (m, 1H; H9), 1.36 (m, 1H; H19), 1.45 (m, 1H; H6), 1.48 (m, 1H; H22), 1.50 (m, 1H; H21), 1.55 (m, 1H; H21), 1.56 (m, 1H; H12), 1.57 (m, 1H; H11), 1.58 (m, 3H, H2(2H), H6 (1H)), 1.62 (m, 1H; H1), 1.63 (m, 1H; H11), 1.71 (m, 1H; H16), 1.72 (m, 1H; H12), 1.979 (s, 3H; Me32), 2.02 (m, 1H; H7), 2.08 (m, 1H; H16), 4.41 (dd, $J = 11.2$, 5.0 Hz; H3), 5.52 ppm (dd, $J = 7.7$, 2.5 Hz; H15); ^{13}C NMR (150 MHz, [D$_6$]acetone): $\delta = 15.62$ (q; C25), 16.95 (q; C24), 18.09 (t; C11), 19.39 (t; C6), 19.83 (q; C27), 21.04 (q; C32), 22.67 (q; C30), 24.17 (t; C2), 26.72 (q; C26), 27.88 (q; C29), 28.27 (q; C23), 29.09 (t; C21), 33.04 (t; C12), 34.54 (s; C17), 36.19 (d; C19), 37.37 (d; C20), 37.44 (q; C28), 38.02 (t; C1), 38.31 (s; C10), 38.59 (s; C4), 39.14 (t; C22), 39.68 (s; C8), 40.81 (s; C13), 41.27 (t; C16), 42.63 (t; C7), 49.88 (d; C9), 56.33 (d; C5), 61.40 (d; C18), 81.17 (d; C3), 117.1 (d; C15), 160.2 (s; C14), 170.9 ppm (s; C31, C=O); MS (EI): m/z (%): 69 (44.3), 81 (35.7), 133 (53.8), 204 (47.7), 269 (60.4), 284 (33.0), 329 (49.3), 344 (100), 468 (11.9) [M^+]; HRMS (EI): m/z calcd for $C_{32}H_{52}O_2$: 468.39673; found: 468.39648.

Data for 20: $[\alpha]_D^{25} = +63.7$ ($c = 0.11$ in $CHCl_3$); solid; ^{1}H NMR (600 MHz, $CDCl_3$): $\delta = 0.789$ (s, 3H; Me30), 0.83 (m, 1H; H5), 0.848 (s, 6H; Me28&Me29), 0.878 (s, 3H; Me19), 0.972 (s, 3H; Me18), 1.00 (m, 1H; H15), 1.06 (m, 1H; H1), 1.10 (m, 1H; H15), 1.33 (m, 1H; H11), 1.34 (m, 1H; H7), 1.37 (m, 1H; H9), 1.42 (m, 1H; H12), 1.44 (m, 1H; H6), 1.50 (m, 1H; H11), 1.51 (m, 1H; H7), 1.53 (m, 1H; H6), 1.604 (s, 3H; Me27), 1.62 (m, 1H; H1), 1.65 (m, 2H; H2), 1.668 (s, 3H; Me26), 1.689 (br s, 3H; Me21), 1.88 (m, 1H; H19), 1.99 (m, 1H; H19), 2.03 (m, 2H; H23), 2.042 (s, 3H; Me32), 2.13 (m, 1H; H16), 2.22 (m, 1H; H16), 2.27 (br d, $J = 15.8$ Hz; H12), 2.31 (br d, $J = 12.1$ Hz; H13), 4.48 (dd, $J = 10.8$, 5.5 Hz; H3), 5.12 ppm (t, $J = 6.9$ Hz; H24); ^{13}C NMR (150 MHz, $CDCl_3$): $\delta = 15.58$ (q; C18), 16.43 (q; C30), 16.44 (q; C19), 16.48 (q; C29), 17.57 (q; C27), 17.60 (q; C21), 18.13 (t; C6), 21.31 (q; C32), 21.57 (t; C11), 23.70 (t; C2), 25.72 (q; C26), 26.07 (t; C23), 27.09 (t; C12), 27.93 (q; C28), 28.70 (t; C16), 30.22 (t; C15), 35.43 (t; C7), 36.99 (s; C10), 37.23 (t; C22), 37.89 (s; C4), 38.73 (t; C1), 39.88 (s; C8), 47.06 (d; C13), 49.53 (s; C14), 50.48 (d; C9), 55.98 (d; C5), 80.93 (d; C3), 124.6 (d; C24), 125.9 (s, C20); 131.2 (s; C25), 136.4 (s; C17), 171.0 ppm (s; C31); the following carbon signals are indistinguishable from each other because they have very similar chemical shifts: Me25/Me26/Me28 and Me29/Me30; MS (EI): m/z (%): 69 (100), 81 (37.7), 93 (56.4), 189 (50.8), 203 (30.7), 297 (9.7), 339 (26.9), 365 (17.4), 393 (11.2), 408 (22.5), 468 (5.0) [M^+]; HRMS (EI): m/z calcd for $C_{32}H_{52}O_2$: 468.39673; found: 468.39710.

Acknowledgements

This work was supported in part by a Grant-in-Aid for Scientific Research from the Japan Society for the Promotion of Science (Nos. 25450150 and 18380001).

[1] For reviews of the polycyclization of triterpene cyclases, see: a) T. Hoshino, T. Sato, *Chem. Commun.* **2002**, 291–301; b) K. U. Wendt, G. E. Schulz, E. J. Corey, D. R. Liu, *Angew. Chem.* **2000**, *112*, 2930–2952; *Angew. Chem. Int. Ed.* **2000**, *39*, 2812–2833; c) G. Siedenburg, D. Jendrossek, *Appl. Environ. Microbiol.* **2011**, *77*, 3905–3915; d) R. A. Yoder, J. N. Johnston, *Chem. Rev.* **2005**, *105*, 4730–4756; e) T.-K. Wu, C.-H. Chang, Y.-T. Liu, T.-T. Wang, *Chem. Rec.* **2008**, *8*, 302–305; f) I. Abe, *Nat. Prod. Rep.* **2007**, *24*, 1311–1331; g) W. D. Nes, *Chem. Rev.* **2011**, *111*, 6423–6451.

[2] R. Xu, G. C. Fazio, S. P. T. Matsuda, *Phytochemistry* **2004**, *65*, 261–291.

[3] a) C. H. Chang, Y. C. Chen, S. W. Tseng, Y. T. Liu, H. Y. Wen, W. H. Li, C. Y. Huang, C. Y. Ko, T. T. Wang, T. K. Wu, *Biochimie* **2012**, *94*, 2376–2381; b) T. K. Wu, C. H. Chang, H. Y. Wen, Y. T. Liu, W. H. Li, T. T. Wang, W. S. Shie, *Org. Lett.* **2010**, *12*, 500–503; c) T. K. Wu, W. H. Li, C. H. Chang, H. Y. Wen, Y. T. Liu, Y. C. Chang, *Eur. J. Org. Chem.* **2009**, 5731–5737; d) T. K. Wu, T. T. Wang, C. H. Chang, Y. T. Liu, W. S. Shie, *Org. Lett.* **2008**, *10*, 4959–4962; e) T. K. Wu, H. Y. Wen, C. H. Chang, Y. T. Liu, *Org. Lett.* **2008**, *10*, 2529–2532.

[4] a) P. Morlacchi, W. K. Wilson, Q. Xiong, A. Bhaduri, D. Sttivend, M. D. Kolesnikova, S. P. T. Matsuda, *Org. Lett.* **2009**, *11*, 2627–2630; b) M. D. Kolesnikova, W. K. Wilson, D. A. Lynch, A. C. Obermeyer, S. P. T. Matsuda, *Org. Lett.* **2007**, *9*, 5223–5226; c) S. Lodeiro, Q. Xiong, W. K. Wilson, M. D. Kolesnikova, C. S. Onak, S. P. T. Matsuda, *J. Am. Chem. Soc.* **2007**, *129*, 11213–11222; d) D. R. Phillips, J. M. Rasbery, B. Bartel, S. P. T. Matsuda, *Curr. Opin. Plant Biol.* **2006**, *9*, 305–314.

[5] a) M. Shibuya, Y. Katsube, M. Otsuka, H. Zhang, P. Tansakul, T. Xiang, Y. Ebizuka, *Plant Physiol. Biochem.* **2009**, *47*, 26–30; b) H. Mitsuguchi, Y. Seshime, I. Fujii, M. Shibuya, Y. Ebizuka, T. Kushiro, *J. Am. Chem. Soc.* **2009**, *131*, 6402–6411; c) M. Shibuya, A. Sagara, A. Saitoh, T. Kushiro, Y. Ebizuka, *Org. Lett.* **2008**, *10*, 5071–5074; d) M. Shibuya, T. Xiang, Y. Katsube, M. Otsuka, H. Zhang, Y. Ebizuka, *J. Am. Chem. Soc.* **2007**, *129*, 1450–1455; e) T. Kushiro, M. Hoshino, T. Tsutsumi, K. Kawai, M. Shiro, M. Shibuya, Y. Ebizuka, *Org. Lett.* **2006**, *8*, 5589–5592.

[6] a) Y. Yonemura, T. Ohyama, T. Hoshino, *Org. Biomol. Chem.* **2012**, *10*, 440–446; b) T. Hoshino, Y. Kumai, T. Sato, *Chem. Eur. J.* **2009**, *15*, 2091–2100; c) N. Morikubo, Y. Fukuda, K. Ohtake, N. Shinya, D. Kiga, K. Sakamoto, M. Asanuma, H. Hirota, S. Yokoyama, T. Hoshino, *J. Am. Chem. Soc.* **2006**, *128*, 13184–13194; d) T. Hoshino, S. Nakano, T. Kondo, T. Sato, A. Miyoshi, *Org. Biomol. Chem.* **2004**, *2*, 1456–1470; e) T. Sato, M, Kouda, T. Hoshino, *Biosci. Biotechnol. Biochem.* **2004**, *68*, 728–738; f) T. Sato, S. Sasahara, T. Yamakami, T. Hoshino, *Biosci. Biotechnol. Biochem.* **2002**, *66*, 1660–1670; g) T. Hoshino, S. Ohashi, *Org. Lett.* **2002**, *4*, 2553–2556; h) T. Hoshino, T. Abe, M. Kouda, *Chem. Commun.* **2000**, 441–442; i) T. Hoshino, T. Sato, *Chem. Commun.* **1999**, 2005–2006; j) T. Hoshino, M. Kouda, T. Abe, T. Sato, *Chem. Commun.* **2000**, 1485–1486; k) T. Hoshino, K. Shimizu, T. Sato, *Angew. Chem.* **2004**, *116*, 6868–6871; *Angew. Chem. Int. Ed.* **2004**, *43*, 6700–6703.

[7] A. Eschenmoser, L. Ruzicka, O. Jeger, D. Arigoni, *Helv. Chim. Acta* **1955**, *38*, 1890–1940.

[8] T. Kushiro, M. Shibuya, K. Masuda, Y. Ebizuka, *J. Am. Chem. Soc.* **2000**, *122*, 6816–6824.

[9] a) R. Ito, Y. Masukawa, T. Hoshino, *FEBS J.* **2013**, *280*, 1267–1280; b) R. Ito, K. Mori, I. Hashimoto, C. Nakano, T. Sato, T. Hoshino, *Org. Lett.* **2011**, *13*, 2678–2681.

[10] a) A. Kawaguchi, H. Kobayashi, S. Okuda, *Chem. Pharm. Bull.* **1973**, *21*, 577–583; b) S. Lodeiro, Q. Xiong, W. K. Wilson, Y. Ivanova, M. L. Smith, G. S. May, S. P. T. Matsuda, *Org. Lett.* **2009**, *11*, 1241–1244; c) M. Kimura, T. Kushiro, M. Shibuya, Y. Ebizuka, I. Abe, *Biochem. Biophys. Res. Commun.* **2010**, *391*, 899–902.

[11] H. Chivers, R. E. Corbett, R. E. M. Mitchell, *J. Chem. Soc. C* **1966**, 1814–1816.

[12] S. Mecozzi, A. P. West, Jr., D. A. Dougherty, *Proc. Natl. Acad. Sci. USA* **1996**, *93*, 10566–10571.

[13] a) D. A. Dougherty, *Science* **1996**, *271*, 163–168; b) a recent review: D. A. Dougherty, *Acc. Chem. Res.* **2013**, *46*, 885–893.

[14] J. A. Faraldos, A. K. Antonczak, V. González, R. Fullerton, E. M. Tippmann, R. K. Allemann, *J. Am. Chem. Soc.* **2011**, *133*, 13906–13909.

Received: May 18, 2013
Revised: August 31, 2013
Published online: November 6, 2013

